On the testing of three-phase equipment under voltage sags

A. Rolán[1], F. Córcoles[2], J. Pedra[2], Ll. Monjo[2] and S. Bogarra[3]

[1] Department of Industrial Systems Engineering and Design-Electrical Engineering Area, University Jaume I, Vicent Sos Baynat Av, Castelló de la Plana 12071, Spain
[2] Department of Electrical Engineering, ETSEIB-UPC, Av. Diagonal 647, Barcelona 08028, Spain.
[3] Department of Electrical Engineering, ETSEIAT-UPC, Colom 1, Terrassa-Barcelona 08222, Spain.

E-mails: rolan@uji.es, corcoles@ee.upc.edu, pedra@ee.upc.edu, lluis.monjo@upc.edu, bogarra@ee.upc.edu

Abstract: This paper provides insight into the testing of three-phase equipment exposed to voltage sags caused by faults. The voltage sag recovers at the fault-current zeros, leading to a *discrete* voltage recovery, i.e., the fault is cleared in different steps. In the literature the most widespread classification divides *discrete* sags into fourteen types. Our study shows that it is generally sufficient to consider only five sag types for three-phase equipment, here called *time-invariant* equipment. As the remaining nine sag types cause identical equipment behaviour in Park or Ku variables, the number of laboratory tests (or of extensive simulations) on equipment under sags is reduced by a ratio of 14/5. The study is validated by simulation of a three-phase induction generator and a three-phase inverter, which are *time-invariant*, and a three-phase diode bridge rectifier, which is not *time-invariant*. Both analytical study and simulation results are validated by testing a three-phase induction motor and a three-phase diode bridge rectifier.

1 Introduction

The voltage in sags caused by faults has a *discrete* recovery. Sags are commonly classified into fourteen types [1]. This paper shows that it is generally sufficient to consider only five *discrete* sag types for grid-connected equipment (e.g., induction and synchronous machines, power inverters or active rectifiers), called *time-invariant* (TI) in this paper. TI equipment meets the following three conditions: (I) the pre-fault dynamic three-phase electrical variables (e.g., the three-phase currents and/or fluxes) are constant when expressed in Park or Ku variables in the synchronous reference frame; (II) if the equipment is controlled, the control strategy is carried out in Park or Ku variables (any reference frame is valid), not in abc phase variables; (III) there is no neutral connection.

The remaining nine sag types lead to identical equipment behaviour in transformed variables (regardless of the reference frame). Thus, the number of experimental tests (or of simulations) on TI equipment under sags is reduced by a ratio of 14/5.

In order to validate the study, a squirrel-cage induction generator, an inverter and a diode bridge rectifier are simulated during voltage sag events. As the diode bridge rectifier does not meet condition I, the grouping of sags is only applicable to the first two devices. The results illustrate that the grouped sags produce identical effects on both.

Finally, both analytical and experimental results are validated by experimental results in the laboratory, where a three-phase induction motor and a three-phase diode bridge rectifier were tested under voltage sags. The experimental results verify the sag grouping proposed in this paper.

2 Voltage sag characterization and classification

A voltage sag is characterized by four parameters [1], namely duration (Δt), depth (h), fault current angle (ψ) and sag type. Note that the sag depth (h) for the symmetrical sags is the remaining voltage with respect to the pre-fault (nominal) voltage, while the sag depth in the unsymmetrical sags is defined by a simple voltage divider on the sequence circuits in radial feeders, as detailed in [2]. In this paper the fault current angle (ψ) equals 80º, which is a typical value for transmission grids.

Sags are mainly caused by faults. Three-phase faults generate symmetrical sags, i.e., type A sags, while one- or two-phase faults generate unsymmetrical sags, i.e., types B, C, D, E, F and G sags. This classification is given in [2] and Appendix 1.

Faults are cleared by the circuit breaker in the natural fault-current zeros, resulting in a *discrete* voltage recovery. Then, faults involving two fault currents, i.e., 1-phase-to-ground or 2-phase faults, are cleared instantaneously (or abruptly) in the affected phases. This is the case of sag types B, C and D. In contrast, symmetrical or unsymmetrical faults involving three fault currents (i.e., three-phase faults or 2-phase-to-ground faults) are cleared in two or three steps, leading to a discrete voltage recovery. Furthermore, these faults can be fully cleared in two different ways. Thus, they lead to sags with two different discrete voltage recovery sequences, i.e., sag types A_1 and A_2 , E_1 and E_2 , F_1 and F_2 and G_1 and G_2 , or sags with three different discrete voltage recovery sequences, i.e., sag types A_3, A_4 and A_5. As a result, the ways to fully clear the faults are classified into fourteen groups [1], five of which refer to symmetrical sags (named A_1, A_2, A_3, A_4 and A_5) while the other nine refer to unsymmetrical sags (denoted as B, C, D, E_1, E_2, F_1, F_2, G_1 and G_2). Appendix 2 shows the *discrete* fault-clearing instants for each sag type and the sag sequence during fault clearance.

The sag classification is simplified if the zero-sequence voltage is removed. Then,

- According to Appendix 1, sag type B is a particular case of sag type D (a sag type D with h = 1/3…1 has the same positive- and negative-sequence voltages as a sag type B with h = 0…1).

- According to Appendix 1, sag types E and G are equivalent as they have identical positive- and negative-sequence voltages.

- According to Appendix 2, sag types A_3 and A_5 are equivalent if the sag sequence during voltage recovery is considered.

Thus, only ten sag types must be studied assuming no zero-sequence voltage: A_1, A_2, A_4, A_5, C, D, F_1, F_2, G_1 and G_2.

The simulated network is based on the voltage divider of a faulted radial network, according to [2]. The grid and fault model used in this manuscript makes the following assumptions:

- The direct- and inverse-sequence components of the source impedances are about equal (the fault is far enough from the electromechanical generators).
- The direct- and inverse-sequence components of the feeder impedances are equal.
- There are different approaches on the zero-sequence impedances for the different sag types, the most restrictive being that the zero-sequence impedance of the source and of the feeder equals the corresponding direct-sequence impedance (solidly grounded system).
- The short-circuit current is sinusoidal and has a constant frequency at every instant, i.e., the voltages before, during and after the fault are sinusoidal with a constant frequency. Only the voltage amplitudes and phase angles change during the event.
- The equipment is connected to the point of common coupling (PCC). The equipment's current does not alter the voltage shape at the PCC.

All simulations and experimental tests in this paper have been made by modelling the voltage seen at the equipment terminals with a controlled voltage source calculated according to the previous assumptions.

Fig. 1 (adapted from [2]) shows the faulted radial network considered in this study. It is assumed that a fault is produced at point F of the feeder, while the considered equipment (induction machine, power converter…) is connected at the point of common coupling (PCC). The circuit breaker (CB) clears the fault and isolates the faulted feeder from the remaining of the network. It is assumed that the considered equipment in this paper remains connected to the network during and after the event.

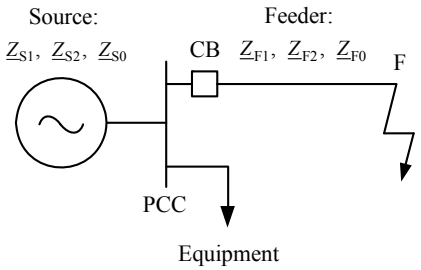

Fig. 1 *Faulted radial network considered in this paper (adapted from [2]).*

3 Sag comparison

The study of sag effects on grid-connected equipment relies on two approaches: to consider or ignore the transformer connections.

3.1 Considering the transformer connections

Let us suppose that a 1-phase-to-ground fault, i.e., a type B sag, occurs in the power system of Table 1. This sag propagates through the different voltage levels, and its profile in abc phase variables is altered by the transformers, as illustrated in that table.

The delta-wye (Dy) and wye-delta (Yd) transformers eliminate the zero-sequence voltage and only modify the phase of the positive- and negative-sequence voltages (they do not alter their modulus if the transformation ratio

is unity). Thus, the Dy and Yd transformers change the sag type. In the example of Table 1, the type B sag is transformed into a type C sag by the first Dy transformer and then into a type D sag by the second Dy transformer. Regarding Dd or Yy transformers, they are equivalent to two cascade Dy transformers. With regard to the sag initiation and clearance instants, t_i and t_{fl}, respectively, the following comments can be made:

- Instant t_i can take any value as the fault can be initiated at any arbitrary instant.

- Instant t_{fl} is defined by the fault clearance process and depends on the faulted phases (type of fault) and the fault current angle, ψ. Thus, this instant is not arbitrary, but can take the discrete values in Appendix 2 only.

Table 1 also shows the modulus and angle of the transformed voltage in the complex plane, v_f, when applying the Ku transformation [3] (v_f is a complex notation for the Park dq components) in the synchronous reference frame. This voltage is calculated as

$$v_f = \frac{1}{\sqrt{2}}\left(v_d + jv_q\right) = \frac{e^{-j(\omega t+\Psi_0)}}{\sqrt{3}}\left(v_a + av_b + a^2v_c\right) \quad (1)$$

where ω is the grid voltage pulsation and Ψ_0 is the transformation angle at instant $t = 0$ s (the transformation angle in the synchronous reference frame is $\Psi = \omega t + \Psi_0$).

Table 1 Type B, C and D sags: location at all voltage levels, abc phasors and time evolution of the transformed voltages (with initial transformation angle, Ψ_0, influence). Sag characteristics: $\Delta t = 2.5T$, $h = 0.1$ or 0.4 and $\psi = 80°$

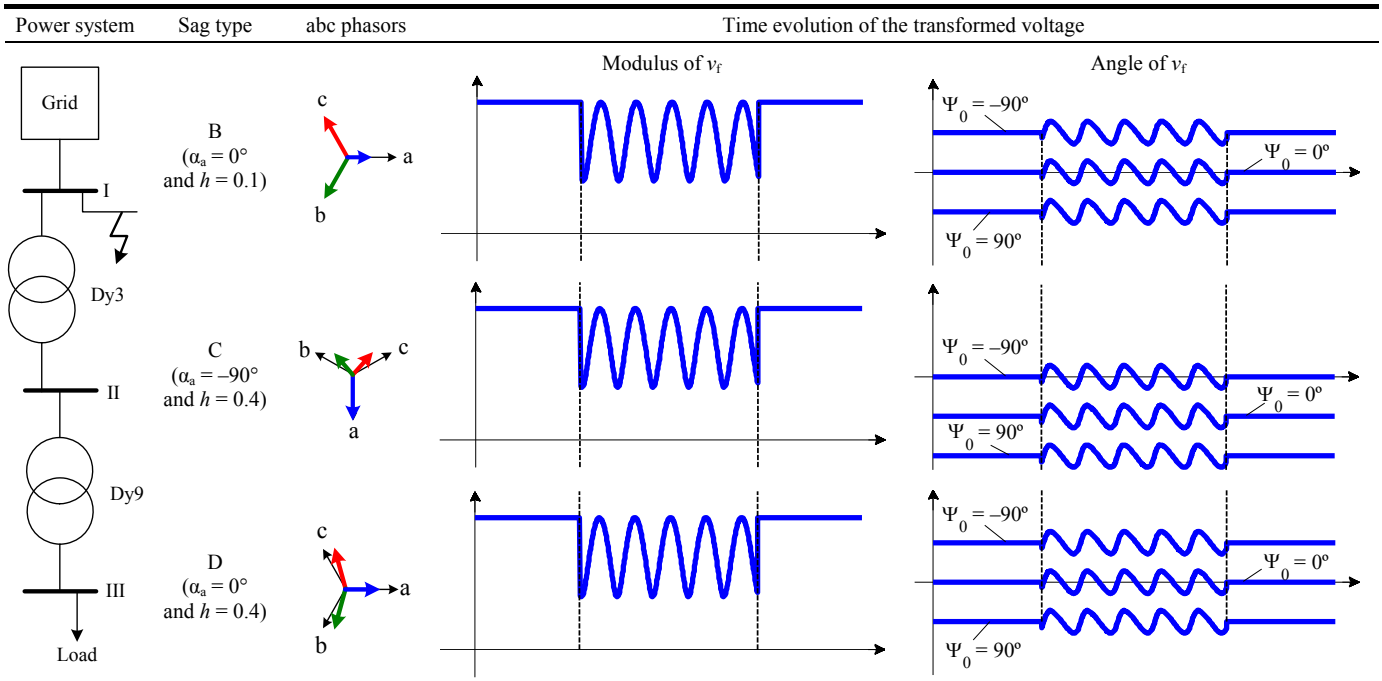

It is worth noting that the Ku variables in the synchronous reference frame are used in the equations and examples in the paper only for simplicity reasons, but neither the use of Park or Ku variables nor the reference frame affects the results.

As can be seen in (1), the transformed voltage v_f depends on Ψ_0, which can be freely chosen. Table 1 shows that this angle does not influence the time evolution of the modulus of v_f but alters the time evolution of the angle of v_f in one offset angle. We will come back to this point in Subsection 4.1.

The results of Table 1 exhibit the following features:

(a) During the fault, the angle of the phase a voltage, α_a, which depends on the transformer clock number and fault type, varies with the voltage levels (for example, $\alpha_a = 0°$ at voltage levels I and III in Table 1 while

$\alpha_a = -90°$ at voltage level II).

(b) As evident, the during-fault voltages (the abc phase and transformed voltages) start and end at the same instants t_i and t_{f1} at all levels.

(c) The time evolution of the modulus of v_f is identical at all voltage levels.

(d) The time evolution of the angle of v_f is identical at all voltage levels by appropriate selection of Ψ_0. For example, the angle of v_f at level II with $\Psi_0 = -90º$ has identical time evolution to that of level III with $\Psi_0 = 0º$. Then, the voltage of the sag type C with $\Psi_0 = -90º$ has identical time evolution to that of the sag type D with $\Psi_0 = 0º$.

3.2 *Ignoring the transformer connections*

In the technical literature sag types are usually modelled without considering the transformer connections (e.g., the sags in Appendix 1). It is further assumed that phasors b and c are symmetrical with respect to phasor a, and α_a is null. Table 2 repeats the sag types of Table 1 but modelled by ignoring the transformer connections: the type C sag is shifted by 90°, while the type B and D sags are maintained as in Table 1.

As α_a in sag type C has been forced to be null, its time evolution in Table 2 exhibits the following changes:

(a) The initial and final instants, t_i and t_{f1}, are time-shifted 90° with respect to those of types B and D.

(b) The time evolution of the modulus and angle of v_f is time-shifted 90° with respect to that of types B and D.

Table 2 Type B, C and D sags when angle shifts due to transformer connections are not considered: abc phasors and time evolution of the transformed voltages (with initial transformation angle, Ψ_0, influence). Sag characteristics: $\Delta t = 2.5T$, $h = 0.1$ or 0.4 and $\psi = 80°$

Sag type	abc phasors	Time evolution of the transformed voltage	
		Modulus of v_f	Angle of v_f
B ($\alpha_a = 0°$ and $h = 0.1$)	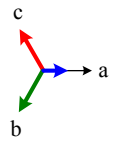	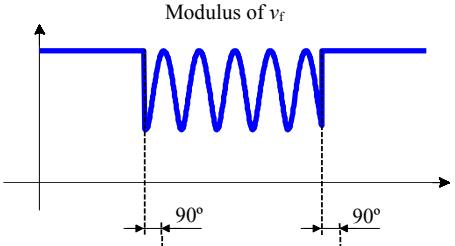	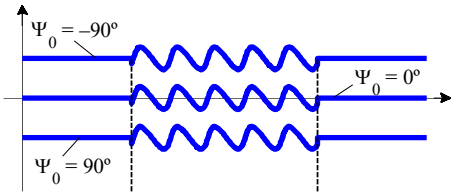
C ($\alpha_a = 0°$ and $h = 0.4$)	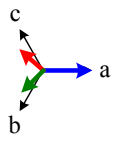	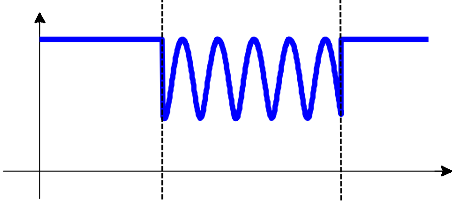	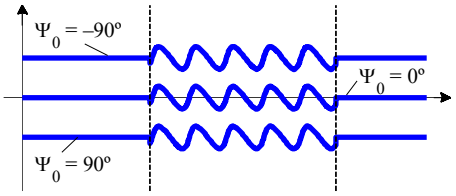
D ($\alpha_a = 0°$ and $h = 0.4$)	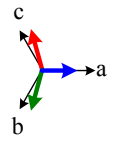	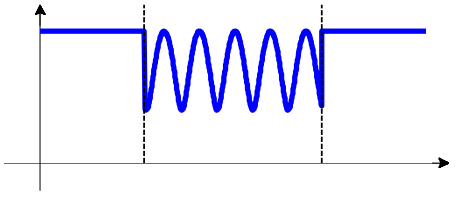	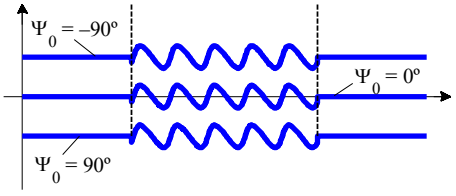

3.3 *Final Remarks*

The aim of the paper is to demonstrate that several pairs of sag types (e.g., C and D) produce identical TI equipment behaviour. Just like the transformed voltages of types C and D only differ in one offset angle in Table 1 (unless Ψ_0 is chosen properly), and one time shift in Table 2, considering or ignoring the transformer

connections is related to the influence of one offset angle (or the Ψ_0 choice) and of one time shift, respectively, on equipment behaviour.

4 Transformed voltage analytical expression

The expression for the transformed voltage of an unsymmetrical sag in the synchronous reference frame is obtained from (1) as

$$v_{\mathrm{f}}(t) = \sqrt{3/2}\left(V_{\mathrm{p}} + V_{\mathrm{n}}\mathrm{e}^{-\mathrm{j}\left(2\omega t+\varphi_{\mathrm{p}}+\varphi_{\mathrm{n}}\right)}\right)\mathrm{e}^{\mathrm{j}\left(\varphi_{\mathrm{p}}-\Psi_0\right)} \tag{2}$$

where V_{p} and V_{n} are the rms value of the positive- and negative- sequence voltages, and φ_{p} and φ_{n} are their angles. The modulus and angle of the transformed voltage (2) are

$$\begin{aligned} |v_{\mathrm{f}}(t)| &= \sqrt{3/2}\sqrt{V_{\mathrm{p}}^2 + V_{\mathrm{n}}^2 + 2V_{\mathrm{p}}V_{\mathrm{n}}\cos\left(2\omega t+\varphi_{\mathrm{p}}+\varphi_{\mathrm{n}}\right)} \\ \alpha_{v_{\mathrm{f}}}(t) &= \left(\varphi_{\mathrm{p}}-\Psi_0\right) + \operatorname{atan}\left(\frac{-V_{\mathrm{n}}\sin\left(2\omega t+\varphi_{\mathrm{p}}+\varphi_{\mathrm{n}}\right)}{V_{\mathrm{p}}+V_{\mathrm{n}}\cos\left(2\omega t+\varphi_{\mathrm{p}}+\varphi_{\mathrm{n}}\right)}\right) \end{aligned} \tag{3}$$

Note that (3) is valid for any unsymmetrical system. As phases b and c are symmetrical with respect to phase a in the sags of Appendix 1, angles φ_{p} and φ_{n} are

$$\varphi_{\mathrm{p}} = \alpha_{\mathrm{a}} \qquad \varphi_{\mathrm{n}} = \alpha_{\mathrm{a}} + \xi\,180^{\mathrm{o}} \tag{4}$$

where ξ is a binary variable equal to 0 or 1 depending on the sag type: $\xi = 0$ for sag types A, C, E and G, and $\xi = 1$ for sag types B, D and F.

Two observations can be made from (3), which agree with the results of Table 1 and Table 2:

1) The transformed during-fault voltage oscillates at a pulsation equal to twice the grid pulsation (2ω).

2) The transformed pre- and post-fault voltage is $v_{\mathrm{f\,PRE\text{-}FAULT}} = \sqrt{3/2}V\mathrm{e}^{\mathrm{j}(\alpha_{\mathrm{a}}-\Psi_0)}$, where $\underline{V} = V\mathrm{e}^{\mathrm{j}\alpha_{\mathrm{a}}}$ is the phasor of the phase a pre-fault voltage. This transformed pre-fault voltage can be chosen as the angle reference for all the transformed variables, i.e., $\Psi_0 = \alpha_{\mathrm{a}}$. For example, the transformed pre-fault voltage at level II in Table 1 is the angle reference for the transformed variables if $\Psi_0 = \alpha_{\mathrm{a}} = -90°$.

4.1 Influence of the initial angle of the transformation (Ψ_0)

Fig. 2*a* illustrates the Ψ_0 influence on the transformation of the abc phase voltages of a type D sag with depth $h = 0.4$, duration $\Delta t = 2.5T$ and angle $\alpha_{\mathrm{a}} = 0°$. It is observed that Ψ_0 only causes an offset in the angle of v_{f}, as said in Subsection 3.1, and does not affect its modulus. The cases with $\Psi_0 = -90°$, 0° and 90° in Fig. 2*a* correspond to the examples of Table 1 and Table 2.

Fig. 2*b* shows the Ψ_0 influence on the inverse-transformation of a given voltage v_{f}. It is observed that the same voltage v_{f} can be related to a type D sag (for $\Psi_0 = 0°$ or 180°), type C sag (for $\Psi_0 = 90°$ or –90°) or other non-defined sags in Appendix 1. As a consequence of this similarity, it is expected that the dynamic behaviour of the studied equipment owing to type C or D sags will be identical in transformed variables. This is studied in detail in Section 5. In practice, the most common values for α_{a} and Ψ_0 are

- $\alpha_{\mathrm{a}} = 0°$, which implies that $\underline{V}_{\mathrm{a}}$ is the angle reference for all phasors.
- $\Psi_0 = \alpha_{\mathrm{a}} = 0°$, which implies that the pre-fault voltage v_{f} is the angle reference for all transformed variables.

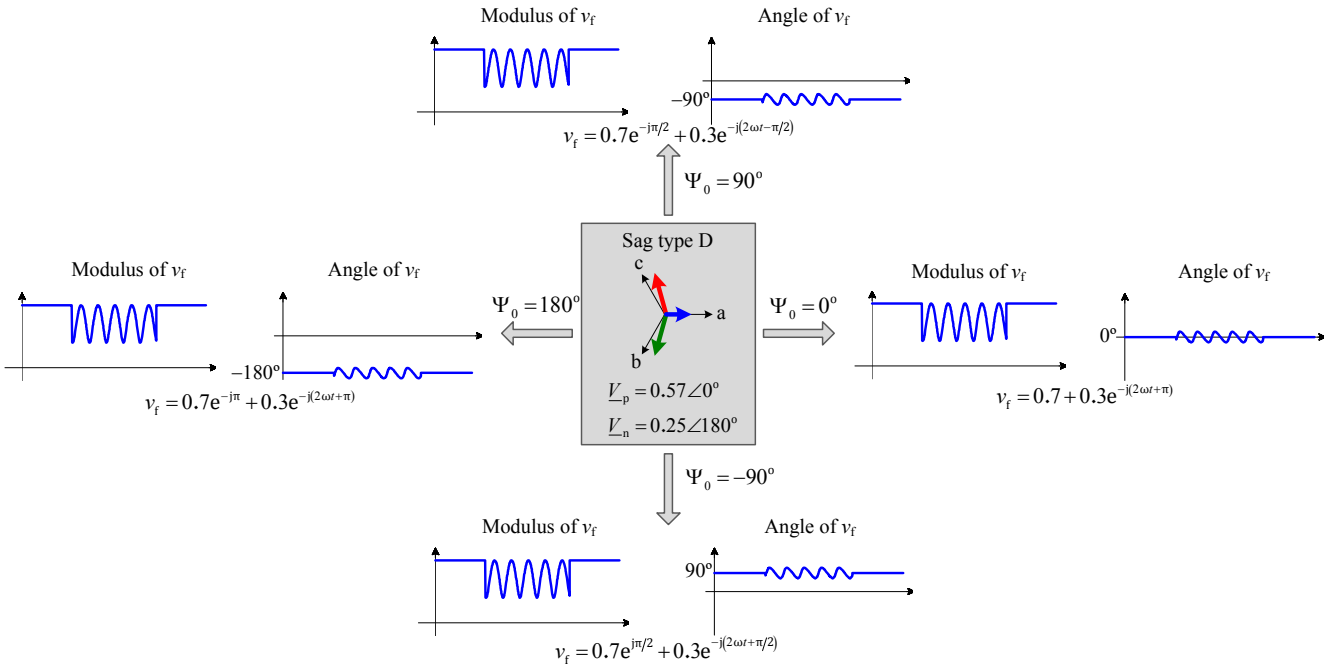

a

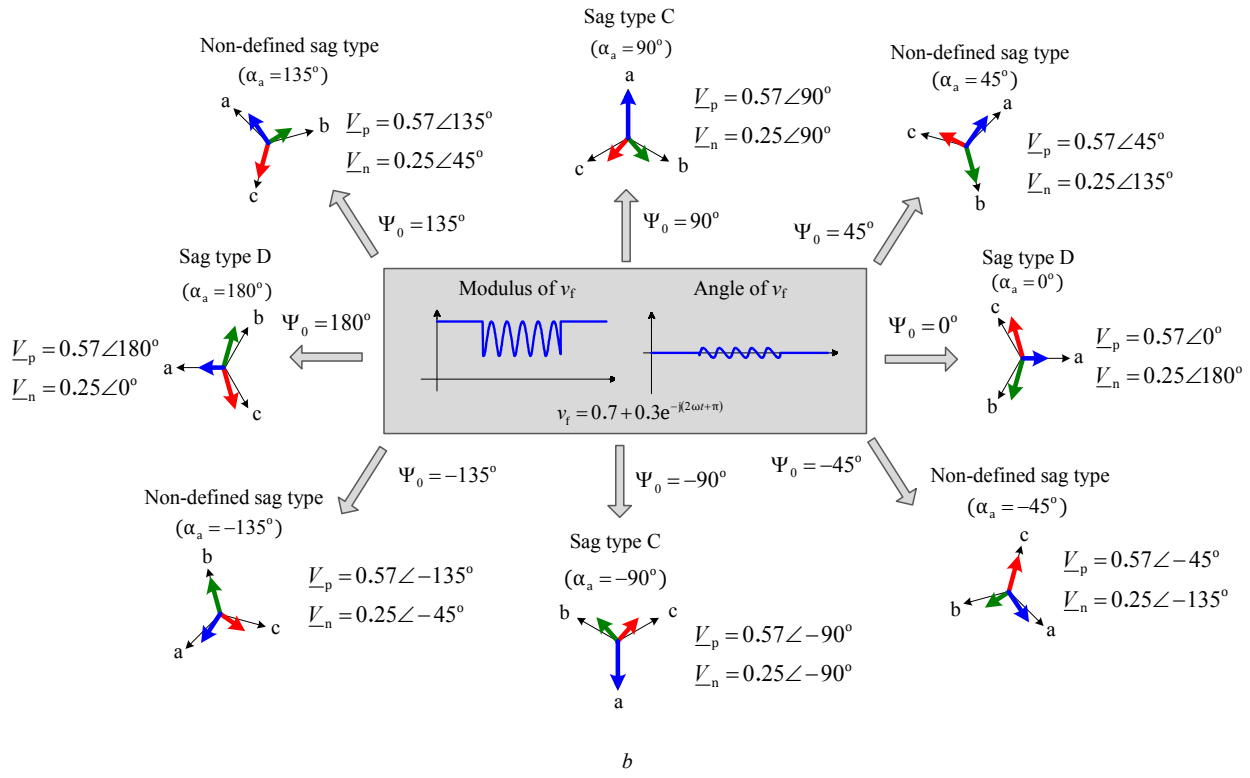

b

Fig. 2 *Influence of the initial transformation angle (Ψ_0)*

a Influence of Ψ_0 on the transformation of a type D sag
b Influence of Ψ_0 on the inverse-transformation of a given voltage v_f
Sag characteristics: $\Delta t = 2.5T$, $h = 0.4$ and $\psi = 80°$

4.2 Grouping of sag types

This subsection analyzes the characteristics of two sags which are different in abc phase variables but identical in transformed variables. Let us assume two unsymmetrical sags 1 and 2, whose positive- and negative-sequence voltages are

$$\begin{aligned} \underline{V}_{\mathrm{p}}^{(1)} &= V_{\mathrm{p}}^{(1)} \angle \varphi_{\mathrm{p}}^{(1)} \qquad & \underline{V}_{\mathrm{n}}^{(1)} &= V_{\mathrm{n}}^{(1)} \angle \varphi_{\mathrm{n}}^{(1)} \\ \underline{V}_{\mathrm{p}}^{(2)} &= V_{\mathrm{p}}^{(2)} \angle \varphi_{\mathrm{p}}^{(2)} \qquad & \underline{V}_{\mathrm{n}}^{(2)} &= V_{\mathrm{n}}^{(2)} \angle \varphi_{\mathrm{n}}^{(2)} \end{aligned} \tag{5}$$

According to (3), both sags have identical transformed voltages $v_{\mathrm{f}}{}^{(1)}$ and $v_{\mathrm{f}}{}^{(2)}$ (i.e., they have identical moduli and angles with identical time evolution) for

$$\begin{aligned} V_{\mathrm{p}}^{(1)} &= V_{\mathrm{p}}^{(2)} \qquad & V_{\mathrm{n}}^{(1)} &= V_{\mathrm{n}}^{(2)} \\ \varphi_{\mathrm{p}}^{(1)} + \varphi_{\mathrm{n}}^{(1)} &= \varphi_{\mathrm{p}}^{(2)} + \varphi_{\mathrm{n}}^{(2)} \qquad & \varphi_{\mathrm{p}}^{(1)} - \Psi_0^{(1)} &= \varphi_{\mathrm{p}}^{(2)} - \Psi_0^{(2)} \end{aligned} \tag{6}$$

If only the first three relations in (6) are satisfied, $v_{\mathrm{f}}{}^{(1)}$ and $v_{\mathrm{f}}{}^{(2)}$ differ in one offset angle. This is the case when considering the transformer connections in sag modelling (Subsection 3.1). If the first two relations in (6) are satisfied but the third is not, the time evolution of $v_{\mathrm{f}}{}^{(1)}$ and $v_{\mathrm{f}}{}^{(2)}$ (modulus and angle) is the same apart from a time shift $\Delta\varphi$ as

$$\Delta\varphi = \left(\varphi_{\mathrm{p}}^{(1)} + \varphi_{\mathrm{n}}^{(1)}\right) - \left(\varphi_{\mathrm{p}}^{(2)} + \varphi_{\mathrm{n}}^{(2)}\right) \tag{7}$$

This is the case when ignoring the transformer connections in sag modelling (Subsection 3.2): e.g., $\Delta\varphi = 90°$ in the type D (or B) and C sags in Table 2. This is also true for the type A_1 and A_2, A_5 and A_4, G_1 and F_1, and F_2 and G_2 sags in Appendix 2, whose time shift is $\Delta\varphi = 90°$ in all cases. These time shifts correspond to differences between the fault-clearing instants $t_{\mathrm{fl}}{}^{(1)}$ and $t_{\mathrm{fl}}{}^{(2)}$ of Appendix 2 and can be mathematically written as

$$\begin{aligned} v_{\mathrm{f}}^{(\mathrm{A}_1)}(t) &= v_{\mathrm{f}}^{(\mathrm{A}_2)}(t + t_{90}) \qquad & v_{\mathrm{f}}^{(\mathrm{A}_5)}(t) &= v_{\mathrm{f}}^{(\mathrm{A}_4)}(t + t_{90}) \qquad & v_{\mathrm{f}}^{(\mathrm{D})}(t) &= v_{\mathrm{f}}^{(\mathrm{C})}(t + t_{90}) \\ v_{\mathrm{f}}^{(\mathrm{G}_1)}(t) &= v_{\mathrm{f}}^{(\mathrm{F}_1)}(t + t_{90}) \qquad & v_{\mathrm{f}}^{(\mathrm{F}_2)}(t) &= v_{\mathrm{f}}^{(\mathrm{G}_2)}(t + t_{90}) \end{aligned} \tag{8}$$

where t_{90} is 1/4 of a period. Note that type G_1 and F_1 sags evolve into type D and C sags, respectively, during fault clearance (see Appendix 2) which, in turn, are also described in (8). The same is true for the type A_1-A_2, A_5-A_4 and F_2-G_2 sags.

As the simplification of considering or ignoring the transformer connections in sag modelling are the same, the next section focuses on the second approach (resulting in a time shift) in order to illustrate the grouping of sag types.

5 Time-invariant equipment

In system theory, a dynamic system is called *time-invariant* (TI) if time-shifting the system input leads to an equivalent time shift in the system output with no other changes [4]. This idea is mathematically expressed as

$$\text{if} \quad u(t) \rightarrow y(t), \quad \text{then} \quad u(t-\tau) \rightarrow y(t-\tau) \tag{9}$$

where $u(t)$ and $y(t)$ are the system input and output, respectively, and τ is the time shift.

Let us define TI three-phase equipment: dynamic three-phase equipment (connected to a balanced network

and operating in sinusoidal steady state) is called TI if the transformed voltage pairs in (8) lead to identical dynamic behaviour with the only change of a 90° time shift in the equipment variables.

In practice, TI equipment is easily recognized if it meets the following three conditions:

(I) The pre-fault dynamic three-phase electrical variables (i.e., the three-phase currents and/or fluxes) are constant if they are expressed in Park or Ku variables in the synchronous reference frame. Note that it is not required to solve the equipment equations in this reference (any reference frame is valid).

(II) If the equipment is controlled (i.e., power inverters and active rectifiers), the control strategy is carried out in Park or Ku variables (any reference frame is valid), not in abc phase variables. For example, the control could be implemented using PI controllers in the synchronous reference frame but also using PR controllers in the stationary reference frame.

(III) There is no neutral connection (i.e., the zero-sequence voltage does not influence equipment behaviour).

Note that the dynamic and control variables related to three-phase magnitudes must be expressed in transformed variables.

In system theory, the transformed voltages in (8) are the TI equipment inputs, while the equipment variables are the outputs whose time shift can be mathematically written as

$$\begin{aligned} &y_{\mathrm{f}}^{(\mathrm{A}_1)}(t) = y_{\mathrm{f}}^{(\mathrm{A}_2)}(t+t_{90}) \qquad y_{\mathrm{f}}^{(\mathrm{A}_5)}(t) = y_{\mathrm{f}}^{(\mathrm{A}_4)}(t+t_{90}) \qquad y_{\mathrm{f}}^{(\mathrm{D})}(t) = y_{\mathrm{f}}^{(\mathrm{C})}(t+t_{90}) \\ &y_{\mathrm{f}}^{(\mathrm{G}_1)}(t) = y_{\mathrm{f}}^{(\mathrm{F}_1)}(t+t_{90}) \qquad y_{\mathrm{f}}^{(\mathrm{F}_2)}(t) = y_{\mathrm{f}}^{(\mathrm{G}_2)}(t+t_{90}) \end{aligned} \tag{10}$$

where y stands for the dynamic variables and any other magnitude expressed in function of the dynamic variables, such as the instantaneous active and reactive powers or the electromagnetic torque.

According to (10), it is sufficient to consider five sag types for the study of sag effects on TI equipment, as types A_1-A_2, A_5-A_4, D-C, G_1-F_1 and F_2-G_2 cause the same time evolution in the transformed dynamic variables.

It is well known that the equations of three-phase induction and synchronous machines with linear magnetic characteristics are linear and time-invariant (LTI) in transformed variables at constant speed and only TI at variable speed. Similarly, averaged models for controlled power converters are usually only TI in transformed variables because of the dc-link voltage control loop. As a consequence, both types of equipment verify the above conditions I and II. Simulation has demonstrated that the following electrical equipment is TI, regardless of the use of Park or Ku variables and the reference frame:

- Three-phase induction (single-cage, double-cage, shorted slip ring or DFIG whose rotor control strategy is implemented in transformed variables) and synchronous (wound rotor or permanent magnet) machines whose output variables are three-phase voltages, currents and fluxes in transformed variables, rotor speed and position, electromagnetic torque, instantaneous active and reactive power, etc.

- Three-phase power inverters and active rectifiers whose control strategy is implemented in transformed variables. The output variables are three-phase voltages and currents in transformed variables, dc bus voltage and current, instantaneous active and reactive power, etc.

- Three-phase passive equipment (linear transformers, capacitor banks, lines, cables and loads) whose output variables are three-phase voltages, currents and fluxes in transformed variables.

Note that the three-phase input/output/control magnitudes of TI equipment are considered in transformed variables (machine and network voltages, currents and/or fluxes). Obviously, the other magnitudes (rotor speed and position, dc bus voltage and current, etc.) are considered in actual values.

6 Simulation examples

In order to validate the study in this paper, three different grid-connected devices under sags are simulated with MATLAB and PSCAD: a three-phase induction generator, a three-phase inverter and a three-phase diode bridge rectifier. Note that only the first two are TI equipment.

6.1 Three-phase induction generator

The 2.3 MW three-phase squirrel-cage induction generator of Table 3, which is driven by a fixed-speed WT, is simulated. Fig. 3 shows the time evolution of the modulus and angle of the transformed stator current, i_{sf}, the rotor speed, ω_m, and the electromagnetic torque, T_e, for the type A_1 and A_2, D and C, and G_1 and F_1 sags.

Table 3 Three-phase squirrel-cage induction generator parameters

Nominal values						Operating point
P_N	U_N	f_N	$\cos(\varphi_N)$	ω_N	T_N	Mech. torque
2.3 MW	690 V	50 Hz	0.89	1512 rpm	14.75 kNm	$T_m = -T_N$
Electrical parameters in pu $(S_b = P_N,\ U_b = U_N)$					Inertia	Pole pairs
r_s	r_r	x_{sl}	x_{rl}	x_m	H	p
$5.60 \cdot 10^{-3}$	$7.20 \cdot 10^{-3}$	0.10	0.10	3.24	2 s	2

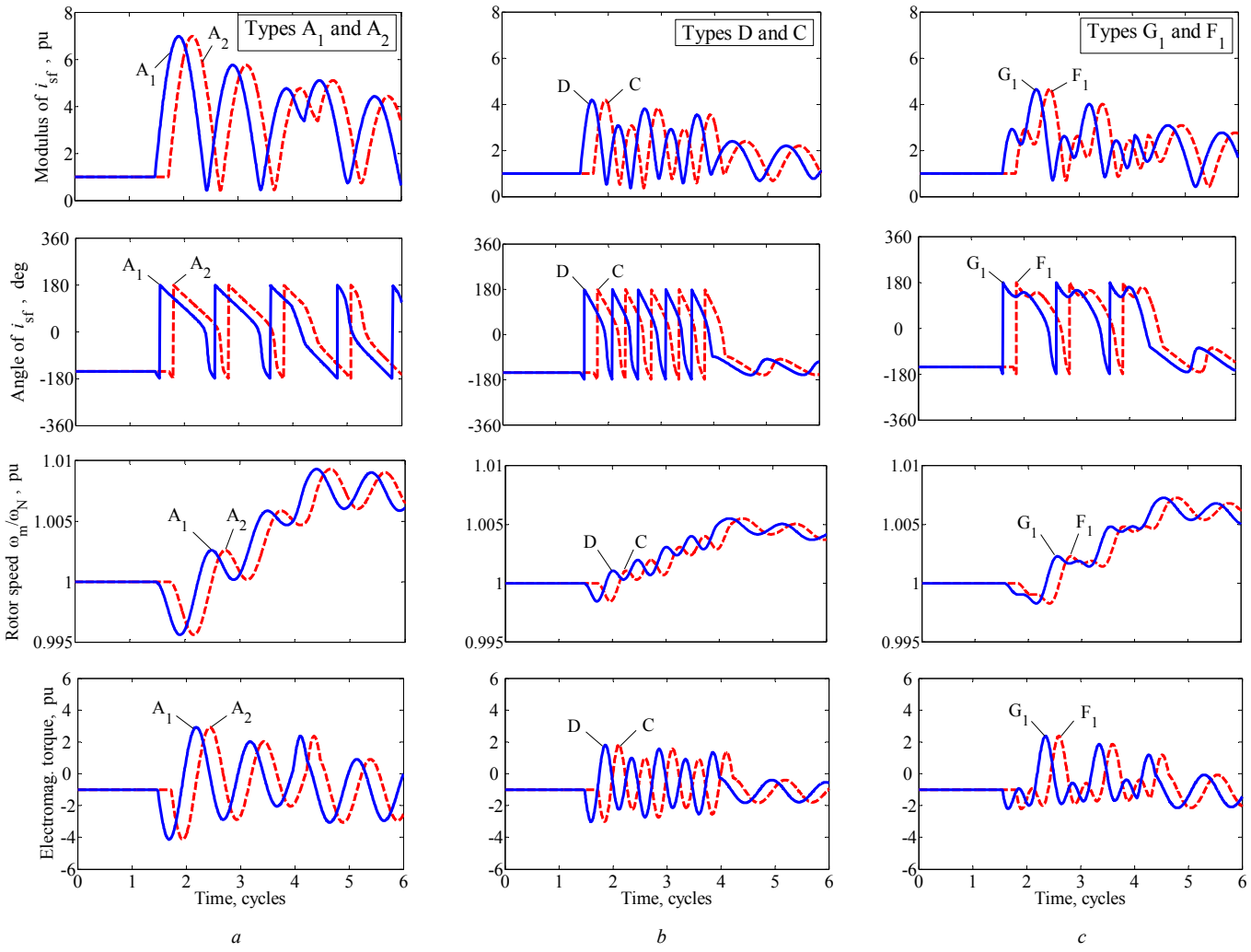

Fig. 3 *Three-phase squirrel-cage induction generator under voltage sags: modulus and angle of the transformed stator current (i_{sf}), rotor speed and electromagnetic torque*

a Sag types A_1 and A_2
b Sag types D and C
c Sag types G_1 and F_1
Sag characteristics: $\Delta t = 2.5T$, $h = 0.1$ and $\psi = 80°$

As can be seen, the time evolution of i_{sf}, ω_m and electromagnetic torque, corresponding to the grouped sag types (A_1-A_2, D-C and G_1-F_1) is identical but time-shifted 90° in all cases. Then, the relations in (10) are satisfied. Note that this is valid not only for the machine dynamic variables (currents and speed), but also for the electromagnetic torque, which is expressed in function of the transformed variables.

6.2 Three-phase inverter

A 0.1 MW grid-connected three-phase inverter whose parameters are given in Table 4 is simulated. The generic structure of the synchronous reference frame control is considered [5]. Although the control is carried out in Park variables (dq components), the simulation results are shown in Ku variables (*forward* component) for clarity purposes. Fig. 4 shows the time evolution of the transformed current (modulus and angle), i_f, injected to the grid. Apart from the inverter switching commutations, it is apparent that the time evolution of the transformed current i_f is the same but time-shifted when the inverter is under the grouped types (A_1-A_2, D-C and G_1-F_1). Then, the relations in (10) are again satisfied.

Table 4 Three-phase inverter parameters

Nominal values				Switch. freq.	DC-link op. point
P_N	U_N	f_N	$V_{dc\,N}$	f_{sw}	I_{dc}
0.1 MW	400 V	50 Hz	900 V	3 kHz	44.4 A
AC-line reactance				DC-link capacitor	
R		L		C	
9.4 mΩ		1 mH		19 mF	

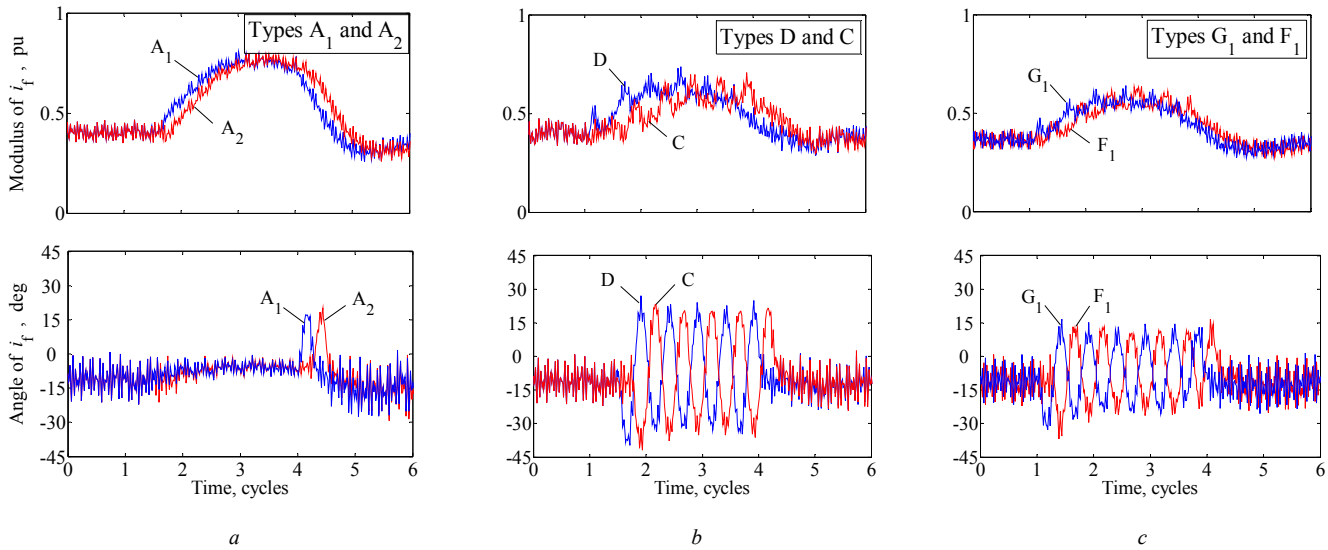

Fig. 4 *Three-phase grid-connected inverter under voltage sags: modulus and angle of the transformed currents injected to the grid (i_f)*

a Sag types A_1 and A_2
b Sag types D and C
c Sag types G_1 and F_1
Sag characteristics: $\Delta t = 2.5T$, $h = 0.6$ and $\psi = 80°$

It is worth noting that the use of an averaged model (neglecting the inverter switching harmonics) would provide an identical time evolution in the transformed currents of the grouped sag types (apart from the well-known time shift).

Finally, although the simple control structure of [5] does not contain independent controls for the positive- and negative-sequence currents occurring during the unsymmetrical sags, it is good enough to illustrate the similarities between the grouped sag types. As the results of this paper are valid for any reference frame, even for the synchronous reference frame of the negative-sequence voltage, the inverters with independent controls for the positive- and negative-sequence currents [6–8] exhibit identical behaviour under the two grouped sag types.

6.3 Three-phase diode bridge rectifier

A three-phase diode bridge rectifier with three line inductors L on the AC-side is simulated [9]. The DC-link consists of a capacitor C connected in parallel to a constant current source I_{dc}. Its parameters and operating point are given in Table 5. Fig. 5 illustrates the time evolution of the modulus and angle of the transformed current, i_f, consumed from the network. Note that this device is not TI equipment as the transformed steady-state pre-fault current i_f is not constant despite having used the synchronous reference frame.

Table 5 Three-phase diode bridge rectifier parameters

Nominal values			DC-link operating point
P_N	U_N	f_N	I_{dc}
10 kW	400 V	50 Hz	18.5 A
AC-line reactance			DC-link capacitor
R		L	C
0 Ω		1.9 mH	1.6 mF

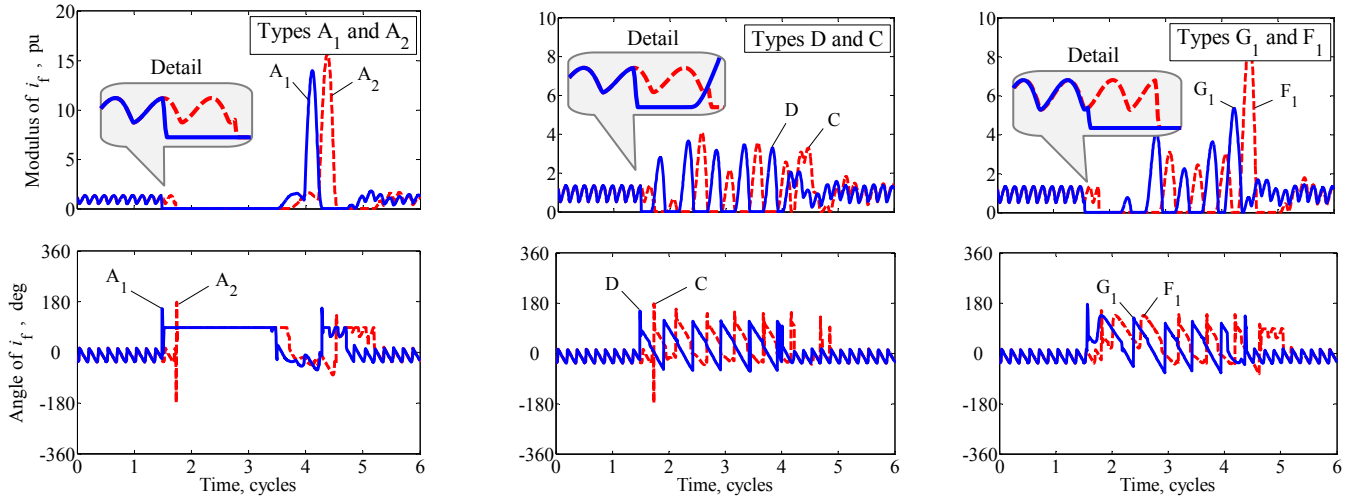

Fig. 5 *Three-phase diode bridge rectifier under voltage sags: modulus and angle of the transformed current absorbed from the grid (i_f)*

a Sag types A_1 and A_2
b Sag types D and C
c Sag types G_1 and F_1
Sag characteristics: $\Delta t = 2.5T$, $h = 0.1$ and $\psi = 80°$

As can be observed in the detail of Fig. 5*a*, the steady-state current i_f takes different values at the initial instants t_i of the type A_1 and A_2 sags, leading to different dynamic behaviours. As a summary, the time evolution of current i_f is different for the grouped sag types (A_1-A_2, D-C and G_1-F_1).

7 Experimental results

In order to validate both the analytical study and the simulation results two different equipments have been tested: a three-phase induction motor (which is a TI equipment) and a three-phase diode bridge rectifier (which is not a TI equipment), whose parameters are given in Table 6 and Table 7, respectively.

Table 6 Parameters of the tested three-phase induction motor

Nominal values				
P_N	U_N	f_N	$\cos(\varphi_N)$	ω_N
2.2 kW	400V	50 Hz	0.78	940 rpm
Electrical parameters in pu ($S_b = P_N$, $U_b = U_N$)				Pole pairs
r_s	r_r	x_{sl}	x_{rl}	x_m	p
0.0352	0.0337	0.0763	0.0763	1.0200	3

Table 7 Parameters of the tested three-phase diode bridge rectifier

Nominal values			AC-line reactance		DC-link capacitor
P_N	U_N	f_N	R	L	C
2.2 kW	400 V	50 Hz	0 Ω	3.9 mH	386 μF

7.1 Three-phase induction motor

The 2.2 kW three-phase squirrel-cage induction motor of Table 6 operates at rated conditions and Fig. 6 shows the time evolution of the modulus and angle of the transformed stator current in the synchronous reference frame, i_{sf}, the rotor speed, ω_m, and the electromagnetic torque, T_e, of the motor when subjected to sag types A_1 and A_2, D and C, and G_1 and F_1. It is observed that this device is a TI equipment as its transformed pre-fault steady-state variables are constant in the synchronous reference frame.

As can be seen from the Fig. 6 results, the time evolution of the variables, corresponding to the sag types A_1-A_2, D-C and G_1-F_1 is identical but time-shifted 90° in all cases. Then, the relations in (10) are satisfied. As a result, it is experimentally demonstrated that sag types A_1-A_2, D-C and G_1-F_1 can be grouped for TI equipments.

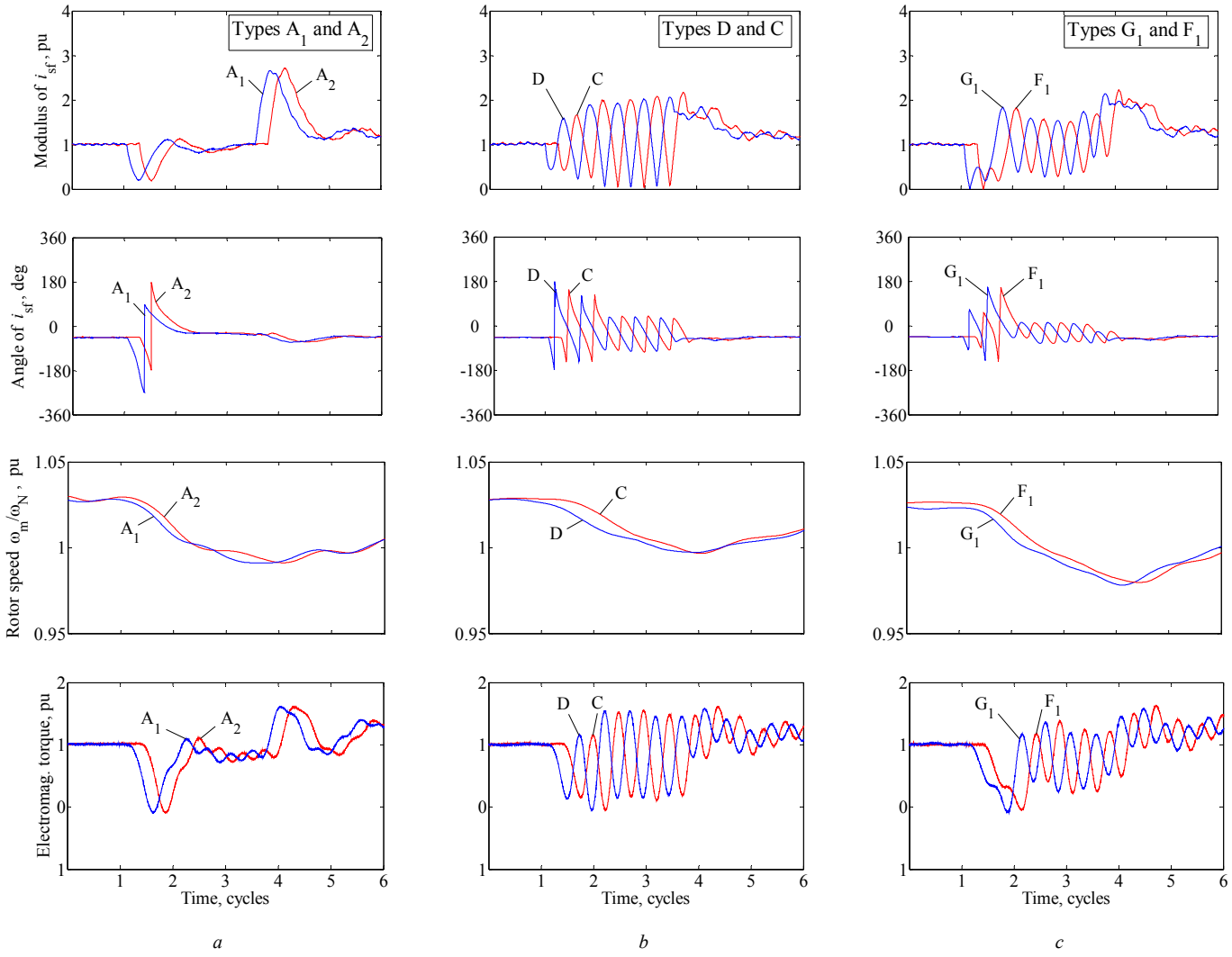

a *b* *c*

Fig. 6 *Three-phase squirrel-cage induction motor tested under voltage sags: modulus and angle of the transformed stator current (i_{sf}), rotor speed and electromagnetic torque*

a Sag types A_1 and A_2
b Sag types D and C
c Sag types G_1 and F_1
Sag characteristics: $\Delta t = 2.5T$, $h = 0.7$ (sag types A_1 and A_2), $h = 0.5$ (sag types D, C, G_1 and F_1) and $\psi = 80°$

7.2 Three-phase diode bridge rectifier

The three-phase diode bridge rectifier of Table 7 operates at rated conditions and Fig. 7 shows the modulus and angle of the transformed current in the synchronous reference frame, i_f, that the rectifier consumes from the network when subjected to sag types A_1 and A_2, D and C, and G_1 and F_1. It is observed that this device is not a TI equipment as the transformed steady-state pre-fault current i_f is not constant in the synchronous reference frame. As a result, the time evolution of current i_f is different for the grouped sag types (A_1-A_2, D-C and G_1-F_1), so the relations in (10) are not satisfied. Then, it is validated experimentally that the previous sags cannot be grouped for non-TI equipments.

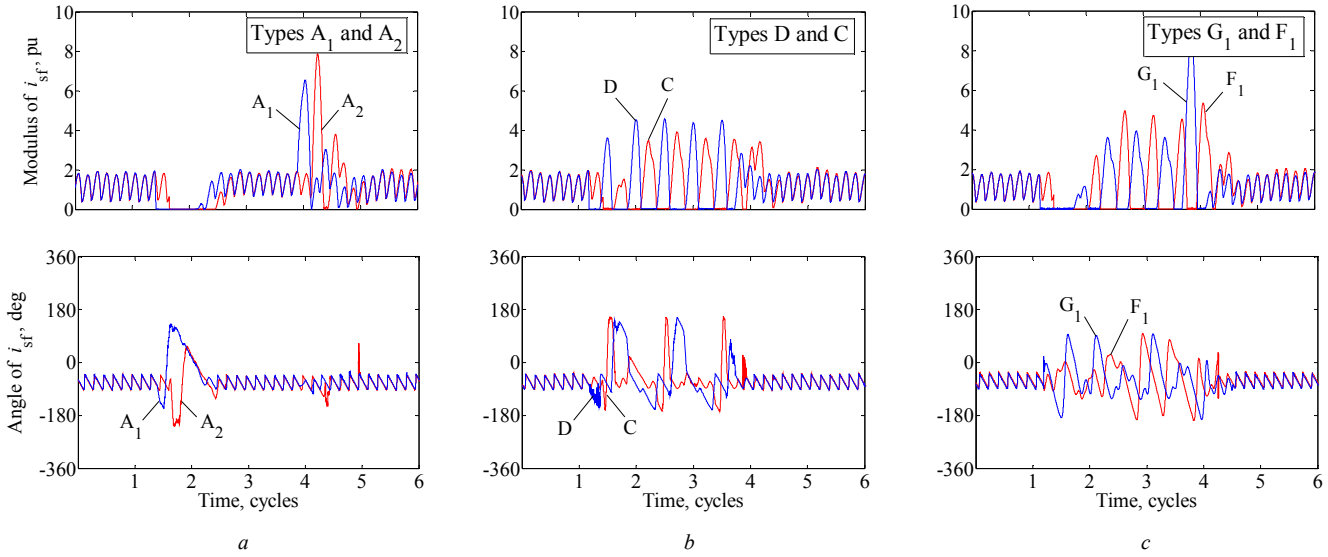

Fig. 7 *Three-phase diode bridge rectifier tested under voltage sags: modulus and angle of the transformed current absorbed from the grid (i_f)*

a Sag types A_1 and A_2
b Sag types D and C
c Sag types G_1 and F_1
Sag characteristics: $\Delta t = 2.5T$, $h = 0.7$ (sag types A_1 and A_2), $h = 0.5$ (sag types D, C, G_1 and F_1) and $\psi = 80°$

7.3 Final Remarks

According to the experimental results shown in Fig. 6 and Fig. 7, we can conclude that the effects of sag types A_1-A_2, D-C, and G_1-F_1 are the same in TI equipments, while they are different for non-TI equipments. Then, the experimental results have perfectly validated both the analytical study and the simulation results of Section 6. As a result, it has been experimentally demonstrated that sag the aforementioned sags can be grouped for TI equipments.

8 Grouping for other sag modelling approaches

Fig. 8 shows three sag modelling approaches which differ in the choice of the voltage recovery instants, t_{f1}, t_{f2} and t_{f3}. Fig. 8*a* illustrates the approach assumed in this paper, which is the most realistic as it takes into account the fault-clearing process (the fault is cleared at instants t_{f1}, t_{f2} and t_{f3} given in Appendix 2 [1]). Fig. 8*c* shows the most usual approach in the literature which, unfortunately, is the least realistic because it considers that the sag ends at any arbitrary instant (i.e., t_{f1} can take any value) and that the fault clearance is *abrupt* (i.e., the fault is cleared instantaneously in all affected phases). As many current laboratory sag generators used for equipment testing are not able to emulate the approach in Fig. 8*a*, the authors propose the intermediate one in Fig. 8*b*. This approach considers that t_{f1} is *discrete* (see Appendix 2) but the fault clearance is *abrupt* (i.e., the fault is cleared instantaneously in all affected phases). The sag grouping proposed for the approach of Fig. 8*a* (A_1-A_2, A_5-A_4, D-C, G_1-F_1 and F_2-G_2) is also valid for that of Fig. 8*b*. Regarding the approach in Fig. 8*c*, the grouping is reduced to sag types A, D-C and G-F, as there are no subtypes for the *abrupt* sag types A, F and G.

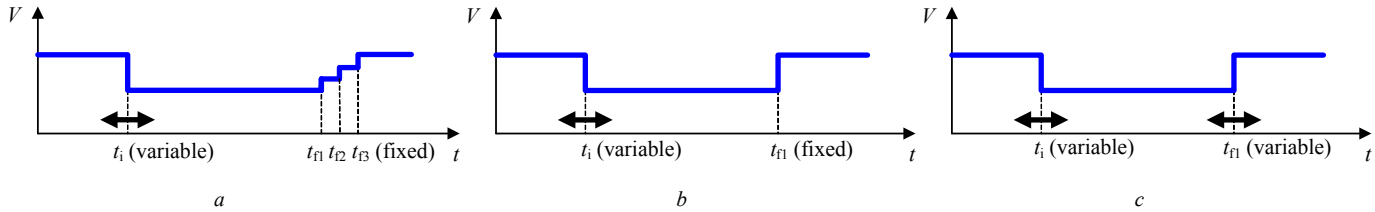

Fig. 8 *Sag modelling approaches. The graphs correspond to the rms voltage during the event (the fault occurs at t_i and is cleared at t_{fl})*

a Fault clearance is *discrete* and voltage recovery occurs at different instants t_{f1}, t_{f2} and t_{f3} (see Appendix 2)
b Fault clearance is *abrupt* in all affected phases and instant t_{f1} can only take a specific value (see Appendix 2)
c Fault clearance is *abrupt* in all affected phases and instant t_{f1} can take any value

9 Conclusions

This study has shown that, among the fourteen *discrete* sag types in the literature, it is generally sufficient to consider only five types for the study of the effects of such disturbances on grid-connected equipment. This is because the following sag types cause identical behaviour in Park or Ku transformed variables: A_1-A_2, A_5-A_4, D-C, G_1-F_1 and F_2-G_2. This means that when analyzing equipment behaviour under voltage sags the number of simulations (or of laboratory tests) is reduced by an approximate ratio of three. This simplification is valid regardless of the reference frame and the use of Park or Ku variables.

The grouping is valid for *time-invariant* (TI) equipment, which is easily recognized because: (I) the pre-fault dynamic three-phase electrical variables (i.e., the three-phase currents and/or fluxes) are constant when expressed in the synchronous reference frame (although the grouping is also valid for any other reference frames), (II) if the equipment is controlled, the control strategy is carried out in Park or Ku variables (any reference frame is valid), not in abc phase variables; (III) the equipment has no neutral connection. Moreover, the grouping is applicable regardless of whether sags are modelled *abrupt* or *discrete*.

The grouping is valid not only for the transformed electrical variables (voltages, currents, fluxes, etc.), but also for the rotor speed, electromagnetic torque and rotor angle in the case of electrical machines, and for any other magnitudes which can be expressed in function of these variables, such as the instantaneous active and reactive powers.

10 Acknowledgements

The authors acknowledge the financial support of the Spanish Ministry of Economy and Competitiveness through project DPI2011-28021.

11 References

1 Bollen, M.H.J.: 'Voltage recovery after unbalanced and balanced voltage dips in three-phase systems', *IEEE Trans. Power Deliv*., 2003, **18**, (4), pp. 1376–1381

2 Bollen, M.H.J.: 'Understanding power quality problems: voltage sags and interruptions' (IEEE Press, New York, 2000)

3 Ku, Y. H.: 'Rotating-field theory and general analysis of synchronous and induction machines', *Proc. IEE–Part IV: Inst. Monogr.*, 1952, **99**, (4), pp. 410–428

4 Oppenheim, A.V., Willsky, A.S., Young, I.T.: 'Signals and Systems' (Prentice-Hall, New Jersey, 1982)

5 Blaabjerg, F., Teodorescu, R., Liserre, M., and Timbus, A.V.: 'Overview of control and grid synchronization for distributed power generation systems', *IEEE Trans. Ind. Electron.*, 2006, **53**, (5), pp. 1398–1409

6 Song, H.S., Nam, K.: 'Dual current control scheme for PWM converter under unbalanced input voltage conditions', *IEEE. Trans. Ind. Electron.*, 1999, **46**, (5), pp. 953–959

7 Gomis-Bellmunt, O., Junyent-Ferré, A., Sumper, A., Bergas-Jané, J.: 'Ride-through control of a doubly fed induction generator under unbalanced voltage sags," *IEEE Trans. Energy Conv.*, 2008, **23**, (4), pp. 1036–1045

8 Teodorescu, R., Liserre, M., Rodríguez, P.: 'Grid converters for photovoltaic and wind power systems' (Wiley, Chichester, 2011)

9 Pedra, J., Córcoles, F., Suelves, F.J.: 'Effects of balanced and unbalanced voltage sags on VSI-fed adjustable-speed drives,' *IEEE Trans. Power Deliv.*, 2005, **20**, (1), pp. 224–233

12 Appendix 1: sequence components of sags

The zero- positive- and negative-sequence components of all sag types are shown in Table 8 (adapted from [2]).

Table 8 Sequence components of sags (from [2])

Type	Zero-sequence	Positive-sequence	Negative-sequence
A	$\underline{V}_{0A}=0$	$\underline{V}_{pA}=h\underline{V}$	$\underline{V}_{nA}=0$
B	$\underline{V}_{0B}=-\left[(1-h)/3\right]\underline{V}$	$\underline{V}_{pB}=\left[(2+h)/3\right]\underline{V}$	$\underline{V}_{nB}=-\left[(1-h)/3\right]\underline{V}$
C	$\underline{V}_{0C}=0$	$\underline{V}_{pC}=\left[(1+h)/2\right]\underline{V}$	$\underline{V}_{nC}=\left[(1-h)/2\right]\underline{V}$
D	$\underline{V}_{0D}=0$	$\underline{V}_{pD}=\left[(1+h)/2\right]\underline{V}$	$\underline{V}_{nD}=-\left[(1-h)/2\right]\underline{V}$
E	$\underline{V}_{0E}=\left[(1-h)/3\right]\underline{V}$	$\underline{V}_{pE}=\left[(1+2h)/3\right]\underline{V}$	$\underline{V}_{nE}=\left[(1-h)/3\right]\underline{V}$
F	$\underline{V}_{0F}=0$	$\underline{V}_{pF}=\left[(1+2h)/3\right]\underline{V}$	$\underline{V}_{nF}=-\left[(1-h)/3\right]\underline{V}$
G	$\underline{V}_{0G}=0$	$\underline{V}_{pG}=\left[(1+2h)/3\right]\underline{V}$	$\underline{V}_{nG}=\left[(1-h)/3\right]\underline{V}$

13 Appendix 2: discrete fault-clearing instants of sags

The discrete fault-clearing instants and the sag sequence during voltage recovery of all sag types are shown in Table 9 (adapted from [1]).

Table 9 Fault-clearing instants of sags (from [1])

Type	1st recovery (ωt_{f1})	2nd recovery (ωt_{f2})	3rd recovery (ωt_{f3})	Sag sequence
A_1	$\kappa - 90°$	κ	—	$A_1 \rightarrow C_a$
A_2	κ	$\kappa + 90°$	—	$A_2 \rightarrow D_a$
A_3	$\kappa - 90°$	$\kappa - 30°$	$\kappa + 30°$	$A_3 \rightarrow E_{2a} \rightarrow B_b$
A_4	κ	$\kappa + 60°$	$\kappa + 120°$	$A_4 \rightarrow F_{2a} \rightarrow C_b^*$
A_5	$\kappa - 90°$	$\kappa - 90°$	$\kappa + 30°$	$A_5 \rightarrow G_{2a} \rightarrow D_b^*$
B_a	$\kappa - 90°$	—	—	—
C_a	κ	—	—	—
D_a	$\kappa - 90°$	—	—	—
E_{1a}	$\kappa + 30°$	$\kappa + 150°$	—	$E_{1a} \rightarrow B_c$
E_{2a}	$\kappa + 150°$	$\kappa - 150°$	—	$E_{2a} \rightarrow B_b$
F_{1a}	$\kappa + 120°$	$\kappa - 120°$	—	$F_{1a} \rightarrow C_c^*$
F_{2a}	$\kappa + 60°$	$\kappa + 120°$	—	$F_{2a} \rightarrow C_b^*$
G_{1a}	$\kappa + 30°$	$\kappa + 150°$	—	$G_{1a} \rightarrow D_c^*$
G_{2a}	$\kappa + 150°$	$\kappa - 150°$	—	$G_{2a} \rightarrow D_b^*$

Notes:

- The angles correspond to voltages expressed by a cosine function. If a sine function is used, the angles must be increased by 90°
- $\kappa = n\,180° - \alpha_a + \psi$, $n = 0, 1, 2\ldots$, α_a = phase angle of phase a voltage
- ψ = fault current angle